



## Flexural Strength and Behavioral Study of High-performance Concrete Beams using Stress-Block Parameters

A. I. A. Momin<sup>\*a</sup>, R. B. Khadiranaikar<sup>b</sup>, A. A. Zende

<sup>a</sup> Department of Civil Engineering, BLDEA's Vachana Pitamaha Dr. P.G Halakatti College of Engineering and Technology Vijayapur, Affiliated to VTU, Belagavi, Karnataka, India

<sup>b</sup> Department of Civil Engineering, Basaveshwar Engineering College, Bagalkot, Affiliated to VTU, Belagavi, Karnataka, India

### PAPER INFO

#### Paper history:

Received 18 August 2021

Received in revised form 13 September 2021

Accepted 23 September 2021

#### Keywords:

Concrete Structures

Strain

Experimental Testing

Structural Element

High-strength Concrete

### ABSTRACT

Most of the existing codes are using stress block parameters which were derived for normal strength concrete. Rectangular stress-block parameters used for normal strength concrete cannot be used safely for higher grade concrete like high-strength concrete (HSC). Hence, new stress-block parameters are established from the experimental investigations. These parameters can be made very much useful in the design of HPC members. Present research aims at behaviour study of HPC using stress block parameters. High performance concrete single span beams were tested under monotonic four-point bending. Considering the experimental stress-strain curves of HPC for grade 60, 80 and 100 MPa, an idealized stress block curve is established and the stress block parameters are derived. Based on the idealized stress block curve, the equations for ultimate moment of resistance, depth of neutral axis, limiting moment of resistance and maximum depth of neutral axis are proposed. Based on the observation of experimental load deformation curves, an ideal load deformation curve is proposed, which follows four significant events identified as, first cracking, yielding of reinforced steel, crushing of concrete with spalling of cover and ultimate failure. The predicted values compare well with the experimental values. The average location of the first crack observed was at 0.535 times the span of the beam from the left support of the observer in the tension zone.

doi: 10.5829/ije.2021.34.11b.18

### NOMENCLATURE

$f_{ck}$	Characteristic strength of concrete	$\epsilon_{cu}$	Ultimate compressive strain
$A_{st}$	Area of tension steel	$f_y$	Characteristic strength of steel
$\rho$	Percentage of tension reinforcement	$M_{ultim}$	Limiting Moment of resistance
$\rho_b$	Balanced reinforcement	$M_{u,pred}$	The predicted ultimate moment of resistance
$\rho/\rho_b$	Longitudinal tension reinforcement ratio	$M_{u,exp}$	experimental ultimate moment
$k_1, k_2$ and $k_3$	Stress factor, Centroid factor and Area factor respectively	$P_u$	Ultimate load at failure of specimen
$x_u$	Depth of neutral axis	$P_f$	Load corresponding to first visible crack
$\bar{x}$	Depth of centre of compression from extreme compression fibre	$\delta_f$	Deflection corresponding to first visible crack
$C_u$	Compressive force	$w_f$	Crack width at failure
$M_u$	Ultimate moment of resistance	$\delta_{s,exp}$	Deflection at service load
$b$	Width of the section	$w_{s,exp}$	Crack width at service load
$d$	Depth of the section	$T_u$	Tension force
$\epsilon_c$	Compressive strain at 85% of ultimate moment	$\epsilon_s$	Tensile strain at 85% of ultimate moment

### 1. INTRODUCTION

The innovation in concrete technology has made use of concrete with increasing compressive strength and hence

special type of concretes like High-Strength Concrete (HSC) and High-Performance Concrete (HPC) were developed. HPC exhibits improved properties for the required performance with long-term serviceability as

\*Corresponding Author Institutional Email:  
[cv.momin@bldeacet.ac.in](mailto:cv.momin@bldeacet.ac.in) (A. I. A. Momin)

compared to conventional concrete and HSC, [1,2]. HPC has many advantages as compared to conventional concrete. HPC could also be advantageously used in the construction of columns, beams, slabs, piles etc. The use of HPC shall result in reduction of structure size, increases available space and also reduce the overall dead loads on the foundation of the structure. HPC can specially be used effectively for structures exposed to severe environments, because of low permeability and high resistance to various environmental factors [3,4]. The results of some of the researchers on conventional concrete in various design codes are not entirely applicable, which are limited to a maximum of 55 MPa strength. It is also not safe and adequate to use the results of conventional concrete having compressive strength less than 55 MPa for designing HPC beams. The flexural behavior of RC structures made of conventional strength concrete is limited due to excessive cracking and deflection, and the structures cast by conventional concrete may later be structurally inadequate. In case of HSC, both early and ultimate strength are higher as compared to conventional concrete. But the durability criteria are not addressed directly in HSC so that it may or may not yield higher durability. As compared to HSC, HPC has improved mechanical properties.

The flexural behavior of reinforced HPC is better compared to reinforced NSC or HSC. Hence, it is essential to investigate the behavior of HPC under flexure. A systematic investigation on the design recommendations of various codes for determination of strength of HPC beams in flexure is essential.

It is seen from the past literature that most of the standard codes are applicable to normal strength concrete, whereas, for higher grades of concrete these methods involving different stress block parameters cannot be extrapolated to use in the design. To study the flexural behavior of HSC, many researchers have proposed stress block parameters validating their experimental results and suggested some major modifications in different codes [5-8]. The stress block parameters are also proposed for special concrete like Geopolymer concrete (GPC) [9]. It is also not known that these stress block parameters proposed for HSC/GPC may or may not be applicable for HPC [10]. The ultimate strain of concrete as suggested by 441-R96 [11] is 0.003 whereas Eurocode-2 [12], Canadian code [13] and Indian Standard Code [14] limits it to 0.0035.

## 2. METHODOLOGY

The present study focuses on investigating the behaviour of single-span reinforced HPC beams experimentally tested under monotonic four-point bending test as shown in Figure 1. The HPC beams are rectangular in cross-section having width of 150mm and effective length of

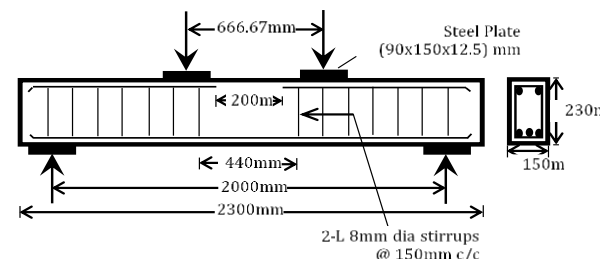


Figure 1. Details of the beam specimen

2000mm. The overall depth of the beam considered was 260mm for 60MPa and 100MPa and 300mm for 80MPa. A total of 12 beams as detailed in Table 1 of single span were cast by varying percentage of longitudinal tension steel, for three compressive strengths of concrete. In order to develop pure flexural behaviour in the beam section, stirrups are not provided between sections having constant moment [15-17]. These beams are grouped as 60SB1, 60SB2, 60SB3 and 60SB4 indicating  $M_{60}$  HPC beams, 80SB1, 80SB2, 80SB3 and 80SB4 indicating  $M_{80}$  HPC beams, 100SB1, 100SB2, 100SB3 and 100SB4 indicating  $M_{100}$  HPC beams.

Firstly, to study the behaviour of HPC beams, idealized stress block curve is established and the stress block parameters were derived. Based on the idealized stress block curve, the equations for ultimate moment of resistance, depth of NA, limiting moment of resistance and maximum depth of Neutral Axis (NA) are predicted for HPC. From the predicted equations, the flexural resistance and NA depth variation are determined and validated with the experimental values. The study also covers the variation of load deformation response and the crack pattern. The beam under investigation were designed using ACI-318 [18] in order to achieve under reinforced section. The beams were loaded and tested as per IS:516-1959 [19]. The testing of beam specimens was carried out for pure flexure test using a loading frame of 2500 kN capacity. The beam at supports and at loading points is provided with steel plate of size 90mm x 150mm x 12.5mm for uniform distribution of stress. The linear variable differential transformer (LVDT's) of gauge length 30mm were attached at the centre of the specimen along the depth of the beam to locate the neutral axis and to measure strains. The deflections of the beam at the centre of the span were also measured by means of LVDT of gauge length 50mm supported over a stand. The load was applied through hydraulic jack and was measured through the load cell of capacity 500 kN. The data were recorded using 24-channel data logger.

## 3. STRESS BLOCK PARAMETERS

Different national codes have different stress block parameters and most of them deal with a compressive

**TABLE 1.** Details of HPC beam specimens in pure flexure for experimental program

Beam Designation	$f_{ck}$	Longitudinal Tension Steel (mm)	$A_{st}$ (mm <sup>2</sup> )	$\rho$	$\rho_b$	$\frac{\rho}{\rho_b}$
60SB1	83.89	2 # 12	226.19	0.78	4.76	0.16
60SB2	85.44	2 # 10+1# 12	270.16	0.93	4.85	0.19
60SB3	84.56	2 # 16+1# 10	480.66	1.69	4.80	0.35
60SB4	85.43	2 # 16+2# 10	559.20	1.97	4.84	0.40
80SB1	89.93	2 # 12 + 1# 10	304.72	0.77	5.10	0.15
80SB2	89.01	3 # 12	339.2	0.86	4.98	0.17
80SB3	87.76	2 # 10+1# 16	358.0	0.91	5.06	0.18
80SB4	89.31	2 # 12+1# 16	427.24	1.09	5.05	0.21
100SB1	105.65	2 # 12	226.19	0.78	5.99	0.13
100SB2	107.25	2#10 + 1# 12	270.16	0.93	6.08	0.15
100SB3	108.12	2 # 16+1# 10	480.66	1.69	6.13	0.27
100SB4	104.34	2 # 16+2# 10	559.20	1.97	5.92	0.33

strength less than 50 MPa. Therefore, an attempt made to derive the stress block parameters for HPC.

From the experimental data, an idealized stress block curve for HPC are established. To arrive at idealized stress block curve for HPC, three strength ranges of concrete are considered. From the behavior observed in experiments, literature survey and graphical representation for each grade of concrete as mentioned above, best fitting polynomial curves were drawn for each grade of concrete as shown in Figure 2. From these curves an idealized stress block curve is derived, which is as shown in the Figure 3. The coefficients such as  $k_1$ ,  $k_3$  and  $k_2$  corresponds to stress factor, area factor and centroid factor, respectively. The value of  $k_1$  is considered on the basis of average of values of stress at ultimate strain and its approximation was verified by literature survey [10]. There is no significant difference in the approximation and values available in the literature. The  $k_3$  and  $k_2$  are derived from assumed stress block and in most cases the approximation of their values holds phenomenally similar to most of literature study.

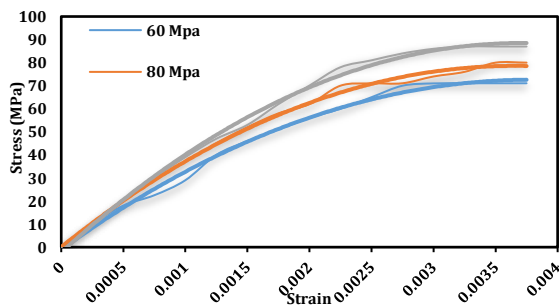


**Figure 2.** Stress-Strain Curve for HPC

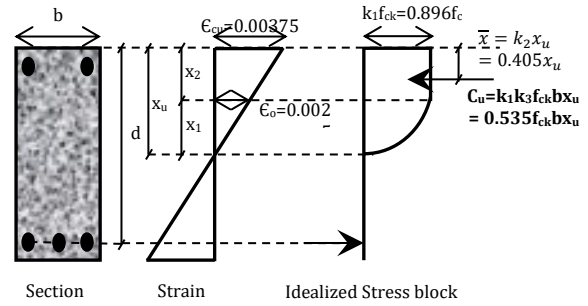


**Figure 3.** Equivalent Stress Block Parameters for Rectangular HPC Sections

Using the strain diagram, the depth  $x_1$  and  $x_2$  are found as

$$x_1 = \frac{2}{3}x_u \text{ and } x_2 = \frac{1}{3}x_u \tag{1}$$

The stress factor  $k_1$  is the average of stresses under ultimate strain observed from experimental results conducted on three different grades of concrete and the area factor  $k_3$  is found by determining the area of stress block and are given by Equation (2).

$$k_1 = 0.896 \text{ and } k_3 = 0.777 \tag{2}$$

The depth of centre of compression fibre is obtained by taking moment of area about extreme fibre as given in Equation (3).

$$\bar{x} = 0.405x_u \tag{3}$$

Thus, from Equation (3), the centroid factor  $k_2$  is given by Equation (4).

$$k_2 = 0.405 \tag{4}$$

Using the coefficients  $k_1$ ,  $k_2$ ,  $k_3$  and considering partial safety factor of 1.3, the total compressive force is obtained as given in Equation (5).

$$C_u = 0.535f_{ck}bx_u \tag{5}$$

The flexural strength of reinforced HPC beam section from the above stress block parameters is obtained by taking moment of  $C_u$  or  $T_u$  as given in Equation (6).

$$M_u = 0.535f_{ck}bx_u(d - 0.405x_u) \tag{6}$$

$$M_u = 0.87f_yA_{st}d \left( 1 - 0.658 \frac{A_{st}f_y}{f_{ck}bd} \right)$$

Finally, the proposed equations and stress block parameters obtained as per the present study are summarized in Table 2.

**TABLE 2.** Proposed Equations and Stress block parameters

Parameter	Equation/ Value
Stress factor $k_1$	$k_1=0.896$
Centroid factor $k_2$	$k_2=0.405$
Area factor $k_3$	$k_3=0.777$

Flexural strength of reinforced HPC beam	$M_u = 0.535f_{ck}bx_u(d - 0.405x_u)$ $M_u = 0.87f_yA_{st}d \left(1 - 0.658 \frac{A_{st}f_y}{f_{ck}bd}\right)$
Depth of NA	$x_u = \frac{0.87f_yA_{st}}{0.535f_{ck}b}$ (7)
Limiting Moment of resistance	$M_{ultim} = 0.1934f_{ck}bd^2$ (8)

#### 4. ULTIMATE STRAIN OF CONCRETE IN COMPRESSION

To measure strain at extreme compression fibre, LVDT was attached at the extreme top fibre at the centre of the HPC beam specimens as shown in Figure 4. The ultimate strain of concrete as suggested by most of the design codes varies from 0.0028 to 0.0035 for strength up to 50 MPa. ACI 441-R96 [11] limits the strain to 0.0030 for both NSC and HSC, but it gives conservative moment capacity for HSC beams, up to 126 MPa strength [20]. As per the findings, the ultimate concrete strain for HSC varies between 0.002 to 0.004 or even higher [17]. The ultimate strain of concrete in compression obtained from the experimental tests is presented in Table 3 for HPC beam specimens for varying HPC strength and longitudinal reinforcement ratio. However, it can be observed from Figure 5, the ultimate strain of concrete obtained are much higher and above the range of specified strain values in Indian Standard Code, ACI code and Euro code. Most of the design codes limit the ultimate strain of concrete to 0.0035, since the ultimate strain of concrete is inversely proportional to compressive strength of concrete. ACI 441-R96 [11] limits the strain to 0.0030 for both NSC and HSC. However, it may not be conservative for higher strength of concrete [11].

This is because of the fact that, as the strength of the concrete increases, the concrete becomes more brittle, and hence takes lesser strain. [21-22]. But, the literature available related to HSC/ HPC are of the view that the ultimate strain is higher than the specified values in design codes. In the present investigation, the specimen tested provided the values much similar to that of available literature on HSC/ HPC. An average ultimate concrete strain of 0.0034, 0.00362 and 0.0038 was obtained for the three ranges of concrete considered in the present investigation.

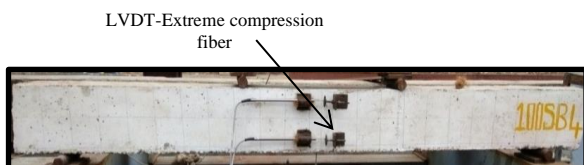


Figure 4. Beam specimen with LVDT to measure ultimate strain for HPC beam specimens

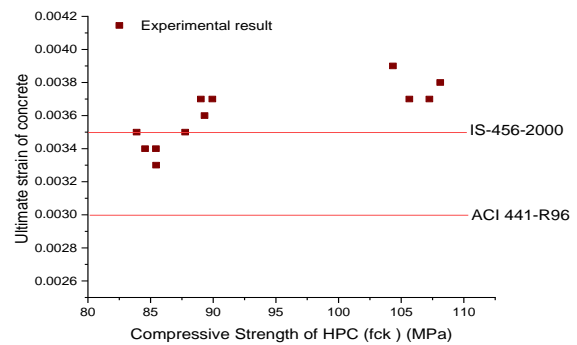


Figure 5. Ultimate strain of concrete for different strength of HPC

#### 5. FLEXURAL RESISTANCE OF HPC BEAMS

The flexural resistance of single span HPC beam specimens tested was predicted by using the stress block parameters developed for HPC. The predicted ultimate moment of resistance ( $M_{u,pred}$ ) determined from Equation (6), is validated with the experimental ultimate moment ( $M_{u,exp}$ ). Table 3 provides the details of strength of concrete, section parameters, percentage of tension reinforcement, ultimate load at failure of specimen, neutral axis and ultimate moment from both experimental and theoretical observations.

The ratio of values of experimental ultimate moment of resistance and theoretical values are determined. It is observed that moment of resistance calculated from stress block curve varies between 0.8 to 1.02 times of experimental values of ultimate moment at failure. Figure 6 indicates the variation of  $M_u/M_{exp}$  ratio with varying percentages of tension reinforcement and characteristic

TABLE 3. Flexural Test results for HPC beam specimens

Beam Designation	D (mm)	$\epsilon_{cu}$	Pu (kN)	$x_u$ (mm)	$M_{u,exp}$ (kN-m)	$M_{u,pred}$ (kN-m)	$M_{u,pred}/M_{u,exp}$
60SB1	191	0.0035	71	15.23	23.67	18.95	0.80
60SB2	192	0.0033	85	17.86	28.33	22.62	0.80
60SB3	189	0.0034	124	32.10	41.53	38.34	0.92
60SB4	189	0.0034	145	36.96	48.50	44.10	0.91
80SB1	261	0.0037	117	19.14	39.30	34.97	0.89
80SB2	261	0.0035	127	21.53	42.33	38.79	0.92
80SB3	262	0.0036	121	23.05	40.33	41.01	1.02
80SB4	261	0.0037	150	27.02	50.13	48.42	0.97
100SB1	191	0.0037	71	12.09	23.83	19.08	0.80
100SB2	192	0.0037	84	14.23	28.17	22.80	0.81
100SB3	189	0.0038	144	25.11	48.23	38.95	0.81
100SB4	189	0.0039	154	30.27	51.53	44.79	0.87

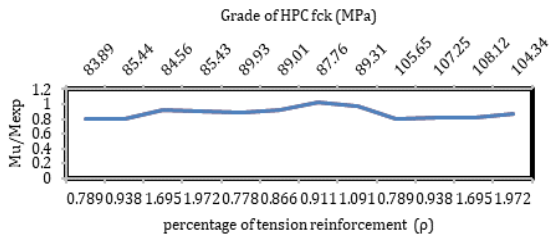


**Figure 6.** Variation of  $M_u/M_{exp}$  with percentage of tension reinforcement and grade of concrete for HPC beam specimens

strength of concrete. The variation of ratio  $M_u/bd^2$  with the percentage of tension reinforcement for both predicted and experimental moment of resistance for first grade of HPC is shown in Figure 7. It can be observed that the variation closely matches the predicted moment of resistance determined from the stress block parameters developed for the HPC. Similar variation is observed for other two strengths.

**6. LOAD DEFLECTION VARIATION**

The experimental load vs deflection curves are presented in Figures 8-10. It was observed that the deformation capacity for some of HPC beams decreased as tension steel reinforcement increased at approximately the same load level.

Thus, it can be proposed that, ductility can be increased by decreasing the tension steel reinforcement as the longitudinal steel reinforcement ratio dominates more than concrete strength. An ideal load-deformation curve considering all the beam specimens is proposed as shown in Figure 11. This curve shows an idealized behaviour of all HPC beams with four distinct segments [23] separated by four significant events, which occurred during the experimental work. These are denoted as A, B, C and D in the ideal curve identified as first cracking, yielding of reinforced steel, crushing of concrete with spalling of cover and ultimate failure, respectively. The

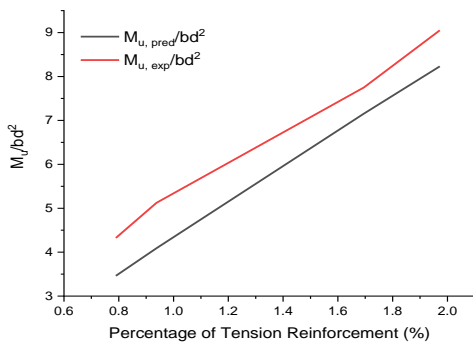


**Figure 7.** Variation of  $M_u/bd^2$  with percentage of tension reinforcement for  $M_{60}$  grade HPC beam specimens

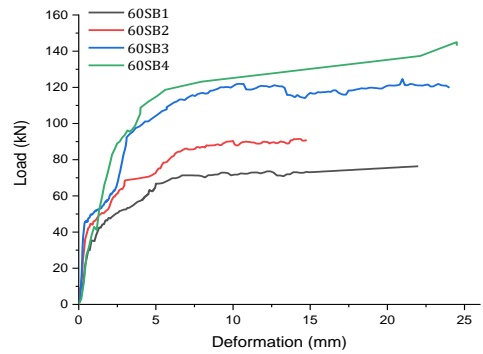


**Figure 8.** Load-deflection curve for  $M_{60}$  grade

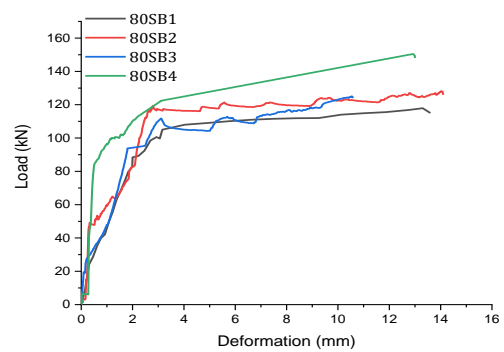


**Figure 9.** Load-deflection curve for  $M_{80}$  grade

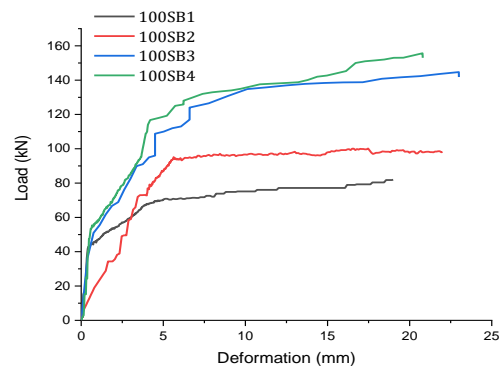


**Figure 10.** Load-deflection curve for  $M_{100}$  grade

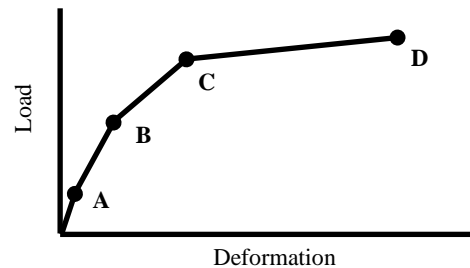


**Figure 11.** Ideal load-deflection curve for HPC beam specimens

zones A and B are due to the reduced beam stiffness while the other two zones cause reduction in the load

applied. A similar behaviour is observed in all the beams. The beam models selected for experimental testing designed as under-reinforced were actually under-reinforced after experimental testing.

The load, deflection and location corresponding to first visible crack and the deflection at failure observed from the experimental testing of beams are presented in Table 4. The location of the first crack is measured with respect to the left support of the observer. It is observed that the load corresponding to first visible crack increased with an increase in the percentage of longitudinal tension steel for the same grade of HPC. The load corresponding to first visible crack also increased for HPC beam specimens. It was also observed that the first crack started in the constant moment zone for all the beam specimens with the average location of 0.535 L from the left support of the observer in the tension zone. Based on the results of Table 4 and from the crack pattern observed for all the beam specimens tested experimentally, the failure started in the tension zone with an average of 81.56% of ultimate load for HPC beam specimens. The first cracking load increased with an increase in the longitudinal reinforcement ratio. On further loading, the crack propagated due to yielding of reinforcing steel followed by crushing of concrete with spalling of cover in compression zone and finally the load carrying capacity was lost with formation of network of cracks.

### 7. CRACK PROPAGATION

The crack pattern and failure modes of HPC beams tested for all the three grades of concrete are shown in Figures 12 to 14. After applying the load on the test specimens, a few hair cracks were observed first and as the load

increased, the first crack appeared in the centre of the specimens at the average location of 0.535 L from the left support. These cracks appeared at the bottom fibres and propagated diagonally towards the top fibres and support. As the load increased, the cracks started propagating towards the supports due to increased shear stress. Many researchers have observed the similar nature of propagation of cracks on high strength beams [23, 25]. As the frequency of loading increased, the micro cracks appeared on the beams fall to macro cracks with crack-width at failure load reaching up to 2.6 mm for the specimen 60SB3.



Figure 12. Crack pattern and failure modes for M<sub>60</sub> grade

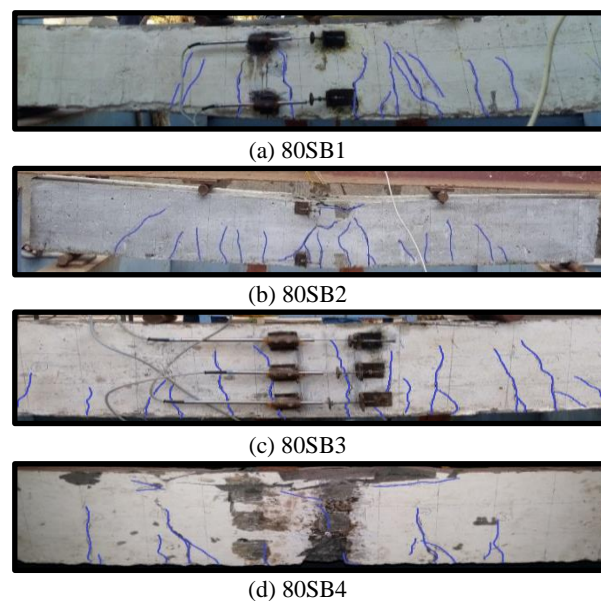
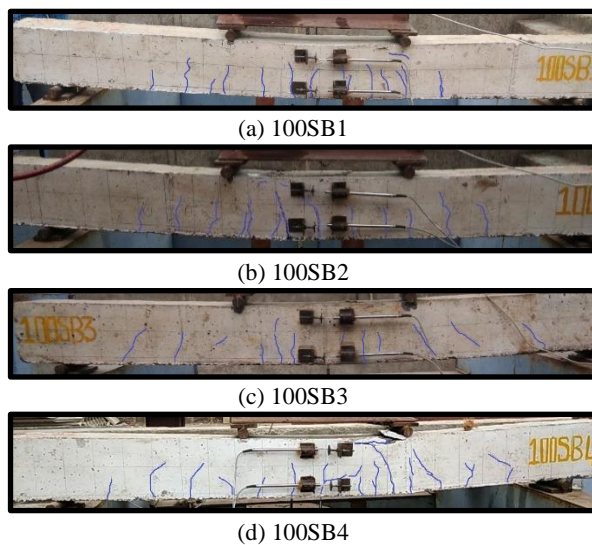


Figure 13. Crack pattern and failure modes for M<sub>80</sub> grade

TABLE 4. Flexural Test results for HPC beam specimens

Beam Designation	P <sub>r</sub> (kN)	δ <sub>r</sub> (mm)	Location	ω <sub>r</sub> (mm)	δ <sub>s, exp</sub> (mm)	ω <sub>s, exp</sub> (mm)
60SB1	66.7	5.00	0.465 L	2.7	1.29	0.45
60SB2	71.4	4.75	0.640 L	2.5	1.42	0.40
60SB3	109	5.70	0.389 L	2.6	2.68	0.45
60SB4	115	5.60	0.677 L	2.1	2.95	0.30
80SB1	105	3.16	0.340 L	2.3	1.77	0.35
80SB2	117	3.30	0.370 L	2.4	1.80	0.35
80SB3	95.3	2.50	0.380 L	2.2	1.45	0.35
80SB4	122	3.10	0.670 L	2.0	0.70	0.30
100SB1	70.3	5.00	0.735 L	1.6	0.41	0.25
100SB2	94.0	6.22	0.660 L	1.4	2.75	0.35
100SB3	124	6.60	0.410 L	1.3	3.13	0.25
100SB4	128	6.23	0.680 L	1.7	3.34	0.30



**Figure 14.** Crack pattern and failure modes for M<sub>100</sub> grade

To obtain the service loads, factor of safety of 1.70 is adopted for the ultimate experimental load [17-18] and the corresponding deflections are obtained. The service load deflections for the tested HPC beams varied from 1.29 to 2.95, 0.70 to 1.80 and 0.41 to 3.34 for strength of 60, 80 and 100 MPa, respectively. The observed deflections are in the range of 0.41 mm to 3.34 mm and are based on only short-term loadings without considering the factors such as shrinkage and creep. The width of the cracks observed at service load during experimental testing ranges from 0.25 to 0.45. The width of the cracks is within the limits as suggested by the design codes at service loads i.e., 2 mm to 5 mm [18].

## 8. CRACK WIDTH

The crack widths observed during the experimental testing at ultimate load are presented in Table 4. During the testing programme, it was observed that all the HPC beams showed vertical cracks or flexural cracks before to failure. The propagation of cracks outside the pure bending zone were also similar to flexural cracks. From Table 4, it is clear that, as the strength of concrete increases the crack widths reduce due to brittle nature of concrete. However, the variation in the crack width was marginal for varying longitudinal tension reinforcement ratio. Hence, strength of the concrete dominated more than the longitudinal tension reinforcement ratio influencing the crack width. The crack widths of HPC beams can be controlled by the longitudinal tension reinforcement. Increase in the usage of mineral admixtures in concrete while producing HPC makes the concrete dense resulting in a stronger interface zone which reduces the cracks [26].

## 9. DEFLECTION AND CRACK WIDTHS AT SERVICE LOADS

The mid-span deflection and crack width at service load from experimental test observations are noted and are presented in Table 4.

## 10. NEUTRAL AXIS DEPTH VARIATION

To study the NA depth variation of HPC, strain-distribution was obtained experimentally at tension reinforcement and at compression zone of concrete. The obtained NA depth from the experimental study is shown in Table 5.

The NA depth was obtained at 85% of ultimate moment. It can be seen from the Table 5, that as the tensile reinforcement ratio increases, the depth of NA also increases for HPC. Considering the cracking load given in Table 4, it was observed that the depth of NA was at mid depth approximately before cracking and just after cracking, the NA depth decreased. At a later stage the NA depth tends to remain the same or decreased slightly. Further, to study the behaviour of NA depth for HPC in more detail, different comparisons were made. The predicted value from the equivalent stress block parameters developed for HPC using Equation (7), is presented in Table 5. From the experimental and predicted results, it can be observed that a lower tensile reinforcement assures a ductile failure for HPC beams for all the three grades of concrete. It can be observed that the experimental NA depth lies in between 0.086 to 0.155 and predicted NA depth lies in between 0.080 to 0.160 for HPC beam specimens. Thus, they are in the same

**TABLE 5.** Flexural Test results for HPC beam specimens

Beam Designation	$X_{pred}/d$	$X_{exp}/d$	$\frac{x_{exp}/d}{x_{umax}/d}$	$\epsilon_c$	$\epsilon_s$
60SB1	0.080	0.086	0.20	0.0030	0.03146
60SB2	0.093	0.097	0.22	0.0028	0.02600
60SB3	0.170	0.181	0.41	0.0029	0.01303
60SB4	0.196	0.188	0.43	0.0029	0.01244
80SB1	0.073	0.082	0.19	0.0031	0.03539
80SB2	0.082	0.096	0.22	0.0030	0.02805
80SB3	0.088	0.091	0.21	0.0031	0.03050
80SB4	0.104	0.108	0.24	0.0031	0.02605
100SB1	0.063	0.069	0.16	0.0031	0.04257
100SB2	0.074	0.076	0.17	0.0031	0.03850
100SB3	0.133	0.137	0.31	0.0032	0.02037
100SB4	0.160	0.155	0.35	0.0033	0.01812

range of, which clarifies that the predicted stress block parameters suit the variation of NA depth for HPC. Many of the researchers have obtained an ultimate strain of more than 0.0035 and as per the present investigation an ultimate strain of 0.00375 was considered for the development of stress block parameters to evaluate the predicted NA depth.

## 11. CONCLUSIONS

Following conclusions are drawn from the experimental investigations carried out on HPC beams produced using locally mineral admixtures

1. The values obtained for ultimate strain from the experimental results are in line with the literature available on HSC. However, most of the design codes suggest values in the range of 0.003 to 0.0036. The ultimate strains of HPC beams strengths investigated seem to be reasonable with these codes.
2. Rectangular stress-block parameters used for NSC cannot be used safely for higher-grade concrete like HPC. Hence, new stress-block parameters are established from the experimental investigations. These parameters can be used in the design of HPC members.
3. Considering the experimental stress-strain curves of HPC for the concrete strengths considered, an idealized stress-block curve is proposed. The equation for moment of resistance of reinforced HPC beams (Equation 6) is derived using the idealized stress block. The moment of resistance of the HPC beam specimens predicted using the proposed equation agree quite closely (12.33% variation) with the experimental flexural strength.
4. Based on experimental load deformation curves, an ideal load-deformation curve is proposed (Figure 11), which follows four significant events identified as, first cracking, yielding of reinforced steel, crushing of concrete with spalling of cover and ultimate failure.
5. The deformation capacity for some of HPC beams decreased as tension steel reinforcement increased at approximately the same load level. Thus, it can be proposed that, ductility can be increased by decreasing the tension steel reinforcement as the longitudinal steel reinforcement ratio dominates more than concrete strength.
6. The width of the cracks observed at service loads during experimental testing was found in between 0.25 to 0.45, and are within the limits as suggested by the design codes. The provisions in some of the design codes overestimate the crack width at service load.
7. The depth of NA for HPC beams increases with increase in the tensile reinforcement ratio. Hence, a lower tensile reinforcement assures a ductile failure for HPC beams for all the three grades of concrete considered.
8. The NA depth are in the same range of (4.65% variation), which clarifies that the predicted stress block

parameters suits the variation of NA depth for HPC beams considered.

## 12. REFERENCES

1. P.C Aitcin, "The durability characteristics of high-performance concrete: A review", *Cement and Concrete Composites*, Vol. 25, No. 4-5 (2003), 409-420, doi: 10.1016/S0958-9465(02)00081-1
2. M. Madhkhan, P. Saeidian, "Mechanical Properties of Ultra High-Performance Concrete Reinforced by Glass Fibers under Accelerated Aging", *International Journal of Engineering, B: Applications*, Vol. 34, No. 05, (2021) 1074-1084, doi: 10.5829/ije.2021.34.05b.01.
3. H. R. Darvishvand, S. A. Haj Seiyed Taghia, M. Ebrahimi, "Utilizing the Modified Popovics Model in Study of Effect of Water to Cement Ratio, Size and Shape of Aggregate in Concrete Behavior", *International Journal of Engineering, B: Applications*, Vol. 34, No. 02, (2021) 393-402, doi: 10.5829/ije.2021.34.02b.11.
4. S. Yasin Mousavi, A. Tavakkoli, M. Jahanshahi, A. Dankoub, "Performance of High-strength Concrete Made with Recycled Ceramic Aggregates", *International Journal of Engineering, Transactions C: Aspects*, Vol. 33, No. 6, (2020), 1085-1093, doi: 10.5829/ije.2020.33.06c.05.
5. Togay Ozbakkaloglu, and Murat Saatcioglu, "Rectangular stress block for high-strength concrete", *ACI Structural Journal*, Vol. 101, No. 4, (2004), 475-483, doi: 10.14359/13333.
6. Karthik, Madhu M., and John B. Mander, "Stress-block parameters for unconfined and confined concrete based on a unified stress-strain model", *Journal of Structural Engineering*, Vol. 137, No. 2, (2010), 270-273, doi: 10.1061/(ASCE)ST.1943-541X.0000294.
7. Abdeldayem, H., Mohamed Hamdy, M., Brahim, B., "Assessing stress-block parameters in designing circular high-strength concrete members reinforced with FRP bars", *Journal of Structural Engineering*, Vol. 144, No. 10, (2018), doi: /10.1061/(ASCE)ST.1943-541X.0002173.
8. Singh, B., Patel, V., Ojha, P. N., Arora, V. V., "Analysis of stress block parameters for high strength concrete", *Journal of Asian Concrete Federation*, Vol. 6, No. 1, (2020), 1-9, doi: 10.18702/acf.2020.6.6.1.
9. Tran, Tung & Pham, Thong, Hao, Hong, "Rectangular Stress-block Parameters for Fly-ash and Slag Based Geopolymer Concrete", *Structures*, Vol. 19, (2019), 143-155, doi: 10.1016/j.istruc.2019.01.006.
10. Oztekin, Ertekin, Selim Pul, and Metin Husem, "Determination of rectangular stress block parameters for high performance concrete", *Engineering Structures*, Vol. 25, No. 3, (2003), 371-376, doi: 10.1016/S0141-0296(02)00172-4.
11. "State of the Art Report on High-Strength Concrete Columns", ACI 441R-1996. American Concrete Institute.
12. "Design of Concrete Structures", Eurocode-2 (1999), European Committee for Standardization, Brussels.
13. "Design of concrete structures", A23.3-94, Canadian Standard Association, Rexdale, Ontario, Canada.
14. "Indian standard code of practice for plain and reinforced concrete for general building construction", IS 456 :2000. Bureau of Indian Standards, New Delhi.
15. Z. R. Aljazaeri, Z. Al-Jaberi, "Numerical Study on Flexural Behavior of Concrete Beams Strengthened with Fiber Reinforced Cementitious Matrix Considering Different Concrete Compressive Strength and Steel Reinforcement Ratio",



- International Journal of Engineering, Transactions A: Basics*, Vol. 34, No. 04, (2021), 793-802, doi: 10.5829/ije.2021.34.04a.05
16. M. Hajsadeghi, M. Jalali, C. Seong Chin, T. Zirakian, M. Bahrebar, "Flexural Characteristics of Fibre Reinforced Concrete with an Optimised Spirally Deformed Steel Fibre", *International Journal of Engineering, Transactions C: Aspects*, Vol. 34, No. 6, (2021), 1390-1397, doi: 10.5829/ije.2021.34.06c.01
  17. P.S. Kumar, M.A. Mannan, V.J. Kurian and H. Achuytha, "Investigation on the flexural behaviour of high-performance reinforced concrete beams using sandstone aggregates", *Building and Environment*, Vol. 42, No. 7, (2007), 2622-2629, doi.org/10.1016/j.buildenv.2006.06.015.
  18. "Building Code Requirements for Reinforced Concrete", ACI 318-1995, American Concrete Institute, Detroit.
  19. "Flexural Strength Test of Concrete", IS 516-1959. Bureau of Indian Standards, New Delhi.
  20. M. A. Rashid and M. A. Mansur, "Reinforced High-Strength Concrete Beams in Flexure", *ACI Structural Journal*, Vol. 102, No. 3, (2005), 462-471.
  21. "State of the Art Report on High-Strength Concrete", ACI 363R-1992, American Concrete Institute, Detroit.
  22. "High Strength Concrete, State of the Art Report", FIP-CEB (1990), CEB Bulletin information No. 197, FIP State of the Art Report SR 90/1, Thomas Telford Ltd, London.
  23. A.A. Momin and R.B. Khadiranaikar, "Experimental and Finite Element Analysis of 80 MPa Two-Span High-Performance Concrete Beam Under Flexure", *Sustainable Construction and Building Materials*, Vol-25, Chapter-35, (2019), 381-396, doi: 10.1007/978-981-13-3317-0\_35.
  24. Samir A. Ashour, "Effect of compressive strength and tensile reinforcement ratio on flexural behavior of high-strength concrete beams", *Engineering Structures*, Vol. 22, No. 5, (2000), 413-423, doi: 10.1016/S0141-0296(98)00135-7.
  25. Swamy, R. N. and Anand, K. L., "Structural behavior of high strength concrete beams", *Building Science*, Vol. 9, No. 2, (1974), 131-141, doi: 10.1016/0007-3628(74)90010-3.
  26. Yang EI, Morita S and Seong TY, "Effect of axial restraint on mechanical behavior of high-strength concrete beams", *ACI Structural Journal*, Vol. 97, No. 5, (2000), 751-756, doi: 10.14359/8810.

---

### Persian Abstract

---

#### چکیده

اکثر کدهای موجود از پارامترهای بلوک تنش استفاده می کنند که برای بتن مقاومتی معمولی استخراج شده است. پارامترهای بلوک تنش مستطیلی که برای بتن مقاومتی معمولی استفاده می شود نمی تواند به طور ایمن برای بتن های درجه بالاتر مانند بتن با مقاومت بالا (HSC) استفاده شود. بنابراین، پارامترهای جدید بلوک تنش از تحقیقات تجربی ایجاد شده است. این پارامترها می توانند در طراحی اعضای HPC بسیار مفید واقع شوند. هدف پژوهش حاضر مطالعه رفتار HPC با استفاده از پارامترهای بلوک تنش است. تیرهای دهانه بتنی با عملکرد بالا تحت خم یکنواخت چهار نقطه ای آزمایش شدند. با در نظر گرفتن منحنی های تنش-کرنش HPC برای درجه ۶۰، ۸۰ و ۱۰۰ مگاپاسکال، منحنی بلوک تنش ایده آل ایجاد شده و پارامترهای بلوک تنش مشتق می شوند. بر اساس منحنی بلوک تنش ایده آل، معادلات لحظه نهایی مقاومت، عمق محور خنثی، لحظه محدود کننده مقاومت و حداکثر عمق محور خنثی ارائه شده است. بر اساس مشاهده منحنی های تغییر شکل بار، یک منحنی تغییر شکل بار ایده آل پیشنهاد می شود که چهار رویداد مهم را شناسایی می کند که عبارتند از: اولین ترک خوردگی، تسلیم فولاد مسلح، خورد شدن بتن با جوش خوردن پوشش و شکست نهایی. مقادیر پیش بینی شده به خوبی با مقادیر تجربی مقایسه می شود. مکان متوسط اولین ترک مشاهده شده ۰.۵۳۵ برابر طول پرتو از سمت چپ ناظر در منطقه کشش بود.

---